Analysis of Contact Force Distribution in a Moving Granule Bed Subjected to Shear Deformation by a Set of Rollers

Graham Calvert[1,2], Hossein Ahmadian[1,2] and Mojtaba Ghadiri[1*]

[1] School of Chemical and Process Engineering, University of Leeds, Leeds, LS2 9JT, UK

[2] Procter & Gamble Technical Centres Ltd, Newcastle upon Tyne, NE12 9BZ, UK

Corresponding author: m.ghadiri@leeds.ac.uk

ABSTRACT

Large contact forces on granules could give rise to undesirable attrition. In a new device, referred to as the Particle Shear and Impact tester, granules are subjected to repeated and sequential impact and shearing, the latter effected by two counter-rotating rollers with differential angular speeds and an adjustable gap between the rollers. This enables the contact force distribution to be varied in order to apply representative contact forces, as experienced in manufacturing plants. Granule flow in the rollers is simulated by Distinct Element Method for several roller gap sizes. The resulting contact force distribution is compared to that from shear cell simulations for representative plant normal stresses (8 to 15 kPa), in order to calibrate the appropriate gap size. The 90th percentile of the contact forces distributions from the two simulations are matched to set the gap size. A roller gap size approximately 3.5 times the 90th percentile of the particle size (based on number distribution) gives a good match of the interparticle contact forces between the rollers and the shear cell. This enables replicating the stresses that granules experience in plants, whether during handling and transport, or during more severe stressing conditions, e.g. compaction or even grinding, thereby assessing attrition or fragmentation propensity of granules.

Keywords: Particle Shear and Impact Tester, Discrete Element Method, Simulation, Contact force distribution, rollers, shearing

1. INTRODUCTION

Granulation and agglomeration of powders using an appropriate binder can provide many attractive attributes that may otherwise be absent in the primary powder, e.g. improved flowability, tabletability, dispersibility in liquids, and mitigation of dust during handling and transport. Tuning the granule properties, such as the mechanical strength, for optimum performance is a subject of great interest in product engineering. A good example is enzyme granules, as their development has had a significant impact in the enhancement of modern detergent formulations. However, their undesirable breakage during transport, handling and processing in manufacturing plants could generate enzyme dust and thereby poses a health risk to plant workers. Therefore, assessment of the predominant mechanical stresses in manufacturing plants and their effect on the breakage of enzyme granules enable manufacturers to produce improved granules and minimise enzyme exposure in such facilities. Ahmadian [1] recognised that the dominant types of stresses experienced by granules in the detergent manufacturing plants were impact and shear deformation. Granule breakage has been extensively investigated and reported in literature, a few examples of which are given in references [2-13]. Ahmadian and Ghadiri [14] used quasi-static single granule compression tests and single granule impact tests to investigate the breakage behaviour of placebo enzyme granules under impact and side crushing forces typical of manufacturing processes. Annular shear cell simulations [15] and rotating drum tests [16] were later used for the same purpose. Ahmadian [1] observed a coupled effect in increasing the extent of breakage when granules underwent a combination of impact and shearing deformation, pointing out a need for a test device that subjects granules to both types of stresses. Thus, the Particle Shear and Impact (PSI) tester has been developed in collaboration with Hosokawa Micron, Runcorn, UK, in order to evaluate granule strength under coupled impact and shear stresses. The device allows for subjecting the granules to multiple impacts at velocities typical of process plants, and sequentially to bulk shear deformation using two counter rotating rollers with an adjustable gap, so that a dense bed of granules moving downwards can be sheared [17].

The focus of the current study is on the rollers of the PSI tester, whose function is to subject a moving dense bed of granules to shear stresses and strains. Granules experience large contact forces through a network of force chains when the moving bed is subjected to shearing strains [13,15,18-21]. The PSI tester is a highly tuneable device which can generate a wide range of contact force distributions by adjusting the gap size. Hence, devising an appropriate criterion to set the gap size requires careful considerations, as the approach differs from compression rollers in which the load is for crushing and/or compaction. The methodology followed here is to set the gap size in the rollers, such that it yields the closest match in the contact force distributions with those in an annular shear cell, with the applied normal loads in the latter being typical of those prevailing in manufacturing plants [14]. In this work, Distinct Element Method (DEM) is used to compare the contact force distribution in a shear box simulation under desired loading conditions to the contact force distribution generated in a roller simulation in order to establish a criterion to set the roller gap size.

2. METHODOLOGY

The PSI tester is fitted with two counter-rotating rollers, which generate a shear band in the granules passing in between them, as described in Table 1. The aim of the rollers is to shear the moving granule bed, having similar contact forces as experienced in a manufacturing plant, by setting an appropriate gap size. Based on the work of Ahmadian [1], the desired shear strain rate that is typical of a detergent manufacturing plant operation is of the order of 20 s^{-1} for which the rotational speed of the rollers can be set using the following equation:

$$\dot{\gamma} \approx \frac{r}{B}\Delta\omega \tag{1}$$

where r is the radius of the rollers, B is the gap size and $\Delta\omega$ is the angular rotational velocity difference between the two rollers (in rads/s). It is difficult to experimentally determine the contact forces acting

on the granules in the nip region for a given gap size. Hence, a computational approach using DEM has been implemented to investigate the effect of the gap size on the contact forces experienced by the moving granular medium. The commercial DEM code PFC3D produced by Itasca Consulting Group, Minneapolis, USA, has been used to perform the simulations. It is based on the application of Newton's second law of motion which determines the translational and rotational motions of each particle arising from the contact and body forces acting upon it. The contact force–displacement law used here is based on the linear spring and dashpot model, as detailed in [24]. Further details of the methodology and approach for setting the gap size are described below.

1. The normal contact force distribution in a simulated shear cell is evaluated first by applying an appropriate normal load to the shear cell and the contact force distribution due to shearing is calculated.

2. A sensitivity study of the rollers gap size is then undertaken in which the contact force distribution is calculated for a number of gap sizes; the appropriate gap size for a given granule is chosen when the contact force distributions prevailing in the shear cell and rollers are similar.

For this study, the properties of three placebo test granule types A, B and C, mimicking three types of commercial enzyme granules, were used, as given in Table 2.

Table 1. Description of the PSI tester rollers.

Table 2. Shear cell simulation parameters and particle properties.

2.1. Shear Cell Simulation Set-up

Shear cell simulations were carried out for the three granule types in order to be used as a reference later, for which the normal contact force distribution under desired stressing conditions was

determined. The simulation is illustrated in Fig. 1. Initially, the shear cell was filled with the desired number of particles by generating spheres in random positions in a larger volume and then allowed to settle under gravity; the bed height was adjusted in a way to ensure the formation of a shear band, following the procedure established previously [13]. Once the bed had settled and the particles were stationary, the lid of the cell was moved downwards to apply a target load. Subsequently, the top half of the cell was moved in the tangential direction and the bed was sheared at a strain rate of 20 s^{-1}, which was the same as the strain rate used in the rollers simulation. The contact force distribution was recorded during the simulation. The particle properties and simulation parameters used are given in Table 2. The normal load applied to each granule system was in the range 8 to 15 kPa, as previously specified by Ahmadian [1], to represent maximum plant stresses for each granule type in a generic enzyme bin.

Fig. 1. Illustration of the shear cell simulation.

2.2. Roller Simulation Set-up

Similar to the shear cell simulation set up, spheres were generated in random positions in a large volume and allowed to fall under gravity in the space between the rollers and the front and back walls. In this case, a horizontal surface was also placed in the roller nip region at time zero to retain them. Once the particles were settled, the holding surface was deleted and simulation was started with the rollers turning. Particles leaving the rollers were recycled back to the top. The same particle properties used in the shear cell simulations were used for the roller simulations (Table 2). For roller simulations, the number of particles was naturally different from the shear cell and depended on the roller gap size. For granule type A, there were 12,079 particles for the simulation of the smallest gap size (0.5 mm) and 16,436 particles for the largest gap size (3.0 mm). For the simulation of granule type B, there were 3,609 particles for the smallest gap size (1.5 mm) and 5,246 particles for the largest gap size (5.0 mm). For granule type C, these were 3,184 and 4,639 particles for the smallest gap size

5

(1.5 mm) and for the largest gap size (5.0 mm), respectively. An illustration of the roller simulation is given in Fig. 2; in this example, the roller on the left is rotating at 13 rpm, whereas the second roller is counter rotating at 21 rpm, giving a velocity difference in the bed for shear deformation. The rollers have the same radius as the experimental rollers and are grooved for effective gripping. The nip region is highlighted in Fig. 2; this is the area of interest for the analysis of contact force distribution, as the particles in this region are subjected to large contact forces, which are more likely to cause particle breakage. The strain rate was fixed at 20 s^{-1} for all simulations and the simulation time was 1 s. The force distribution was exported every 25 ms.

Fig. 2. Illustration of the roller simulation.

3. SIMULATION RESULTS AND DISCUSSION

3.1. Shear Cell Simulation

In Fig. 3, a typical shear cell normal contact force distribution is shown for different strain values. For zero shear strain, i.e. before shearing where no tangential traction has yet been applied, the normal contact force distribution is the smallest. Once the bed is sheared and strain increases, the normal contact force increases. However, it is typically observed that the sheared bed force distribution quickly reaches steady state with little fluctuation, as the shear strains of 0.42 and 0.57 almost overlap. .

Fig. 3. Example of a typical shear cell normal contact force distribution.

The normal contact force for all contacts within the assembly is logged from which its distribution is obtained. The 10th, 50th and 90th percentiles of the normal contact force distribution for

the shear cell simulations are plotted as a function of strain and shown in Fig. 4 for granule type A and in Figs A1 and A2 of Appendix for granule types B and C, respectively. The 50th and 90th percentiles have remarkably little variations at steady shear straining, as the strain rate is fixed at 20 s^{-1}. As shown later, the intention here is to provide the best match in contact force distribution between the shear cell and roller conditions, for which the 90th percentile of the distributions is used. This is summarised in Table 3 for the three granule types. The normal loads of 13.1, 14.7 and 8.4 kPa have been chosen for granule types A, B and C, respectively, to account for differences in particle size and density in order to yield representative plant stresses. Under such conditions and considering the particle properties as given in Table 2, the 90th percentile of the contact force distributions are 30, 180 and 100 mN for granule types A, B and C, respectively. The significance of this approach is that realistic granule attrition per unit shear strain should be obtained for each granule type under simulated plant stresses.

Fig. 4. The 10th, 50th and 90th percentiles of the normal contact force distribution in the shear cell as a function of strain for granule type A (normal stress = 13.1 kPa).

Table 3. The 90th percentile of the contact force distribution for granule types A, B and C subjected to normal loads of 13.1, 14.7 and 8.4 kPa, respectively.

3.2. Roller Simulation

A sensitivity study based on the roller gap size was carried out for each granule, the results of which are given below. Similar to the shear cell simulations, the normal contact force distribution was evaluated and the force was plotted as a function of strain for the three granule types. The results for granule type A are presented below while those for types B and C are given in the Appendix.

As mentioned in Table 1, the number of particles between the rollers is recommended to be greater than 2.2 and less than 6, based on which the gap sizes were selected, depending on the average particle size. Seven gap sizes were investigated for granule type A: 0.5, 1.2, 1.5, 1.75, 2.0, 2.5, and 3.0 mm. The 10th, 50th and 90th percentiles of the normal contact force distribution as a function of strain for granule type A, at a roller gap size of 1.5 mm, are displayed in Fig. 5. Compared to the shear cell, the rollers were simulated for a greater length of time and hence strain. The rationale behind this is that the contact force distribution in the rollers fluctuates considerably more than that in the shear cell. This is attributed to transient jamming in the small gap, and the nature of the rollers, i.e. roller curvature; as the particles are fed through the system, they may align in such a way that leads to mechanical arching. Once these jammed particles break free, the contact force drops, as observed in Fig. 5 at strain of 10 as an example.

Fig. 5. The 10th, 50th and 90th percentiles of the normal contact force distribution in the rollers as a function of strain for granule type A (gap size = 1.5 mm).

The 90th percentile of the normal contact force distribution as a function of strain for all the investigated gap sizes is shown in Fig. 6. Evidently, as the gap size is increased, the contact force decreases noticeably, and the deviation about the mean increases significantly. This is because the rollers grip the moving particle bed in the nip region. As the gap size is increased, the frequency of mechanical arching (i.e. transient jamming) goes down [25], thereby decreasing the normal contact force.

Fig. 6. The 90th percentile of the normal contact force distribution in the rollers as a function of strain for granule type A for all the investigated gap sizes.

In order to determine the roller gap size most representative of the desired stress condition (see Table 2), the roller simulation force plots should be compared to a relevant shear cell simulation. Consequently, the 90th percentiles of the normal contact force distribution from the two simulations are chosen for comparison using the following equation:

$$DF = \frac{F_{90,rollers}}{F_{90,Shear\ Cell}} \tag{2}$$

where DF is dimensionless force, $F_{90,Rollers}$ and $F_{90,Shear\ Cell}$ are the 90th percentiles of the normal contact force distribution from the roller simulation and the shear cell simulation, respectively. As previously discussed, the shear cell normal contact force distributions remain essentially constant with strain. Therefore, $F_{90,Shear\ Cell}$ is considered constant for each granule type and calculated as the average 90th percentile of the normal contact force distribution from the relevant shear cell simulation, as given in Table 3. The reason for using Eq. 2 is to determine which gap size has a dimensionless force closest to unity in order for it to be taken as the desired gap size. As an example, for granule type A, the plot of DF as a function of strain is shown in Fig. 7 for gap sizes 1.2 and 1.5 mm. When the gap size is 1.2 mm, the normalised force, DF, fluctuates around unity. However, at times it is greater than two, which could lead to a greater amount of breakage than expected. Thus, the desired gap size should lead to a DF that approaches unity without surpassing it. Accordingly, for simulated granule type A, a gap size of approximately 1.5 mm should be used. The results for granule types B and C are given in the Appendix. Compared to granule type A, granule type B had a larger particle size distribution and thus slightly larger gap sizes were selected for this test granule type: 1.5, 2.3, 2.5, 3.5, 4.0 and 5.0 mm. For granule type C, a total of seven roller gap sizes were investigated: 1.5, 2.5, 2.7, 3.1, 3.5, 4.0 and 5.0 mm, as it had the largest particles and consequently the largest gap sizes were used for this test granule type. The recommended gap size to keep DF around unity is concluded to be approximately 2.5 mm for granule type B and between 2.7 and 3.1 mm for granule type C.

3.3. Relating Gap Size to Particle Size

From the simulation data reported here, it is possible to relate the gap size to particle size in order to get the desirable contact force distribution. Here, the maximum recorded dimensionless force from each roller simulation is used, so as not to exceed the 90th percentiles of the normal contact force distribution of the shear cell. This measure is taken to avoid subjecting the granules to contact forces larger than necessary, thereby causing unrealistically large extents of attrition. The maximum *DF* is plotted as a function of the relevant normalised gap size, as shown in Fig. 8. The normalised gap size is defined in the following equation:

$$Normalised\ Gap\ Size = \frac{Roller\ Gap\ Size}{d_{p,90}} \tag{3}$$

where $d_{p,90}$ is the 90th percentile of particle diameter number distribution. The gap size is normalised by the larger particles present in the distribution, due to the fact that these particles, when in the nip region of the rollers, are most effective in causing jamming, and may experience a greater extent of breakage. Considering Fig. 8, it appears that the data almost collapse into a single curve. Therefore, it is deemed that a constant normalised gap size could be used for the adequate operation of the PSI tester. Thus, with regards to Fig. 8, the proposed gap size is about 3.5 times the 90th percentile of the particle diameter distribution (by number) when testing granules for their attrition propensity. In both shear cell and rollers tests, strong force chains are involved in jamming and therefore responsible for surface damage and, in case of weak granules, fragmentation. The above analysis indicates that the proposed gap size could simulate the conditions prevailing in manufacturing plants for assessing the tendency of dust formation for a newly developed granule product.

4. CONCLUSIONS

A DEM investigation has been carried out to simulate the required rollers gap size that is necessary for subjecting granules to desired stressing conditions that prevail in manufacturing plants during handling of granules (normal stress of approximately 1-20 kPa). The analysis involved a comparison of the normal contact force distribution that existed in a shear box simulation, under desired loading conditions, to the normal contact force distribution generated in a roller simulation. It is concluded that a gap size of approximately 3.5 times the 90th percentile particle size (based on number distribution) is required when operating the experimental rollers in order to generate similar contact force distribution to that in a shear cell. The use of the rollers makes it possible to subject a bed of granules to continuous shearing while the contact force distribution in the bed can be tuned by adjusting the gap size between the rollers. This enables the PSI tester to replicate the stresses that granules experience in plants, whether during handling and transport, or during more severe stressing conditions, e.g. compaction or even grinding, thereby assessing attrition or fragmentation propensity of granules, thereby assessing attrition or fragmentation propensity of granules.

REFERENCES

[1]   H. Ahmadian, Analysis of enzyme dust formation in detergent manufacturing plant, PhD Thesis, University of Leeds, 2008.

[2]   K.R. Yüregir, M. Ghadiri, R. Clift, Observations on impact attrition of granular solids, Powder Technol. 49 (1986) 53–57. doi:10.1016/0032-5910(86)85004-5.

[3]   A.D. Salman, C.A. Biggs, J. Fu, I. Angyal, M. Szabó, M.J. Hounslow, An experimental investigation of particle fragmentation using single particle impact studies, Powder Technol. 128 (2002) 36–46. doi:10.1016/S0032-5910(02)00151-1.

[4]   W.J. Beekman, G.M.H. Meesters, T. Becker, A. Gaertner, M. Gebert, B. Scarlett, Failure mechanism determination for industrial granules using a repeated compression test, in: Powder Technol., Elsevier, 2003: pp. 367–376. doi:10.1016/S0032-5910(02)00238-3.

[5]   A.D. Salman, J. Fu, D.A. Gorham, M.J. Hounslow, Impact breakage of fertiliser granules, Powder Technol. 130 (2003) 359–366. doi:10.1016/S0032-5910(02)00237-1.

[6]   S. Antonyuk, M. Khanal, J. Tomas, S. Heinrich, L. Mörl, Impact breakage of spherical granules: Experimental study and DEM simulation, Chem. Eng. Process. Process Intensif. 45 (2006) 838–856. doi:10.1016/j.cep.2005.12.005.

[7]   Y.S. Cheong, C. Mangwandi, J. Fu, M.J. Adams, M.J. Hounslow, A.D. Salman, A Mechanistic

Description of Granule Deformation and Breakage, in: Handb. Powder Technol., 2007: pp. 1055–1120. doi:10.1016/S0167-3785(07)12029-7.

[8]   B.J. Ennis, Theory of Granulation: An Engineering Perspective, in: D.M. Parikh (Ed.), Handb. Pharm. Granulation Technol., Informa Healthcare, 2010: pp. 44–47.

[9]   R. Boerefijn, M. Ghadiri, P. Salatino, Attrition in Fluidised Beds, in: Handb. Powder Technol., 2007: pp. 1019–1053. doi:10.1016/S0167-3785(07)12028-5.

[10]   M. Ghadiri, Particle Impact Breakage, in: K. Higashitani, H. Makino, S. Matsusaka (Eds.), Powder Technol. Handb., Fourth edi, CRC Press, 2019.

[11]   B.K. Paramanathan, J. Bridgwater, Attribution of solids-I. Cell Development, Chem. Eng. Sci. 38 (1983) 197–206. doi:10.1016/0009-2509(83)85002-7.

[12]   C.E.D. Ouwerkerk, A micro-mechanical connection between the single-particle strength and the bulk strength of random packings of spherical particles, Powder Technol. 65 (1991) 125–138. doi:10.1016/0032-5910(91)80175-I.

[13]   M. Ghadiri, Z. Ning, S.J. Kenter, E. Puik, Attrition of granular solids in a shear cell, Chem. Eng. Sci. 55 (2000) 5445–5456. doi:10.1016/S0009-2509(00)00168-8.

[14]   H. Ahmadian, M. Ghadiri, Analysis of enzyme dust formation in detergent manufacturing plants, in: Adv. Powder Technol., VSP BV, 2007: pp. 53–67. doi:10.1163/156855207779768188.

[15]   H. Ahmadian, A. Hassanpour, S.J. Antony, M. Ghadiri, Mechanical failure of grains in sheared granular media: Effect of size ratio, AIP Conf. Proc. 1145 (2009) 867–870. doi:10.1063/1.3180067.

[16]   H. Ahmadian, A. Hassanpour, M. Ghadiri, Analysis of granule breakage in a rotary mixing drum: Experimental study and distinct element analysis, Powder Technol. 210 (2011) 175–180. doi:10.1016/j.powtec.2011.03.013.

[17]   H. Ahmadian, M. Ghadiri, Granule attrition by coupled particle impact and shearing, Advanced Powder Technology, 32 (2021) 204-210. https://doi.org/10.1016/j.apt.2020.12.001.

[18]   Z. Ning, M. Ghadiri, Distinct element analysis of attrition of granular solids under shear deformation, Chem. Eng. Sci. 61 (2006) 5991–6001. doi:10.1016/j.ces.2006.03.056.

[19]   C.L. Hare, M. Ghadiri, R. Dennehy, A. Collier, Particle breakage in agitated dryers, in: AIP Conf. Proc., AIP, 2009: pp. 851–854. doi:10.1063/1.3180062.

[20]   M. Ghadiri, Z. Ning, Effect of shear strain rate on attrition of particulate solids in a shear cell, in: Proc. Int. Conf. Powders Grains, Powders & Grains 97, Durham, NC, 1997.

[21]   S.J. Antony, Link between single-particle properties and macroscopic properties in particulate assemblies: Role of structures within structures, Philos. Trans. R. Soc. A Math. Phys. Eng. Sci. 365 (2007) 2879–2891. doi:10.1098/rsta.2007.0004.

[22]   W.A. Beverloo, H.A. Leniger, J. van de Velde, The flow of granular solids through orifices, Chem. Eng. Sci. 15 (1961) 260–269. doi:10.1016/0009-2509(61)85030-6.

[23]   C.C. Crutchley, J. Bridgwater, Particle attrition in small clearances, KONA Powder Part. J. 15 (1997) 21–31. doi:10.14356/kona.1997007.

[24]   G. Clavert, A. Hassanpour, M. Ghadiri, Mechanistic analysis and computer simulation of the aerodynamic dispersion of loose aggregates, Chemical Engineering Research and Design 89 (2011) 519-525. https://doi.org/10.1016/j.cherd.2010.08.013.

[25]   R.P. Behringer, B. Chakraborty, The physics of jamming for granular materials: a review, Reports on Progress in Physics, **82** (2019), 012601.

APPENDIX

Fig. A1. The 10th, 50th and 90th percentiles of the normal contact force distribution in the shear cell as a function of strain for granule type B (normal stress = 14.7 kPa).
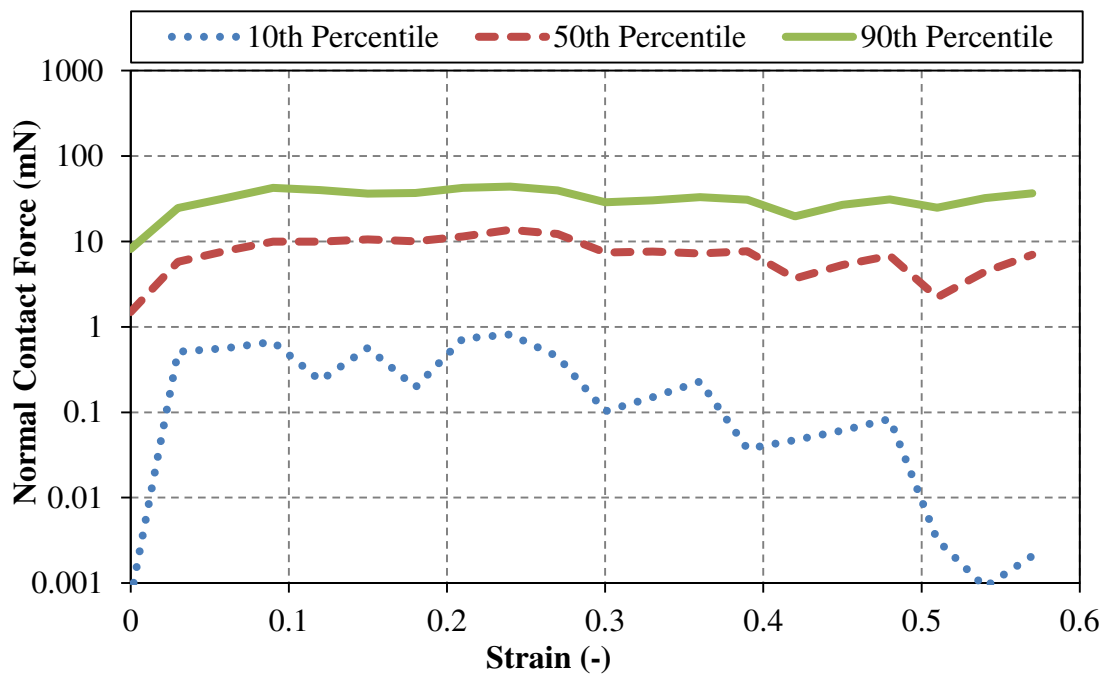
Fig. A2. The 10th, 50th and 90th percentiles of the normal contact force distribution in the shear cell as a function of strain for granule type C (normal stress = 8.4 kPa).

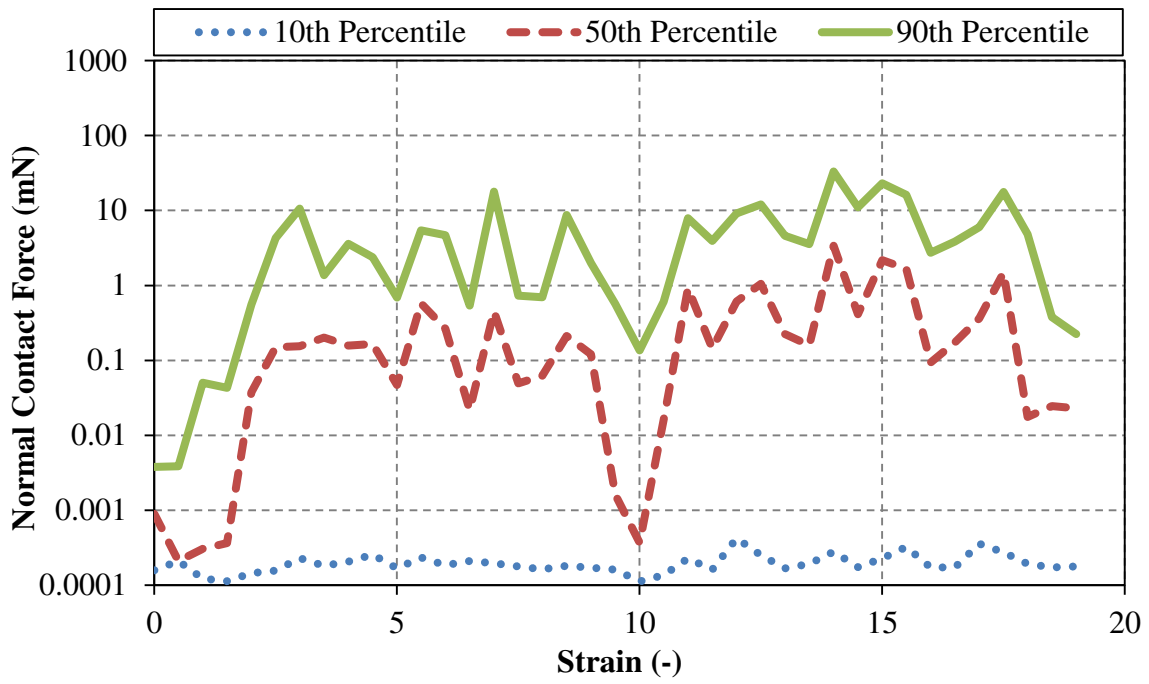Fig. A3. The 90th percentile of the normal contact force distribution in the rollers as a function of strain for granule type B for all the investigated gap sizes.

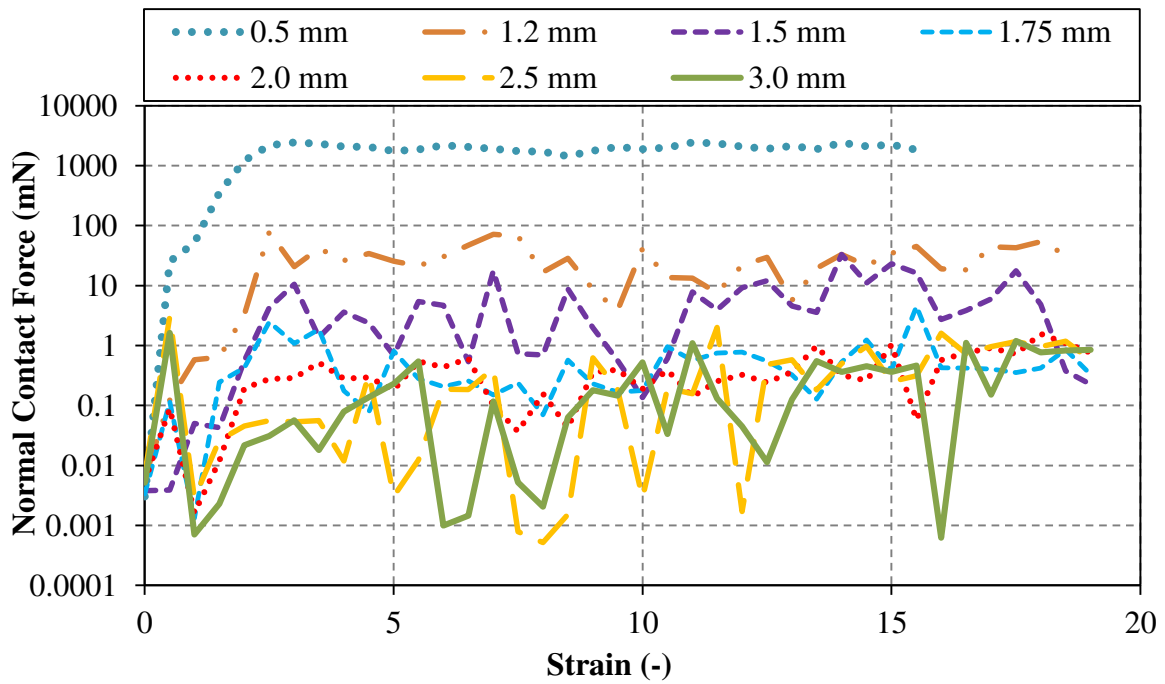Fig. A4. DF as a function of strain for granule type B at gap sizes 2.3 and 2.5 mm.

Fig. A5. The 90th percentile of the normal contact force distribution in the rollers as a function of strain for granule type C for all the investigated gap sizes.
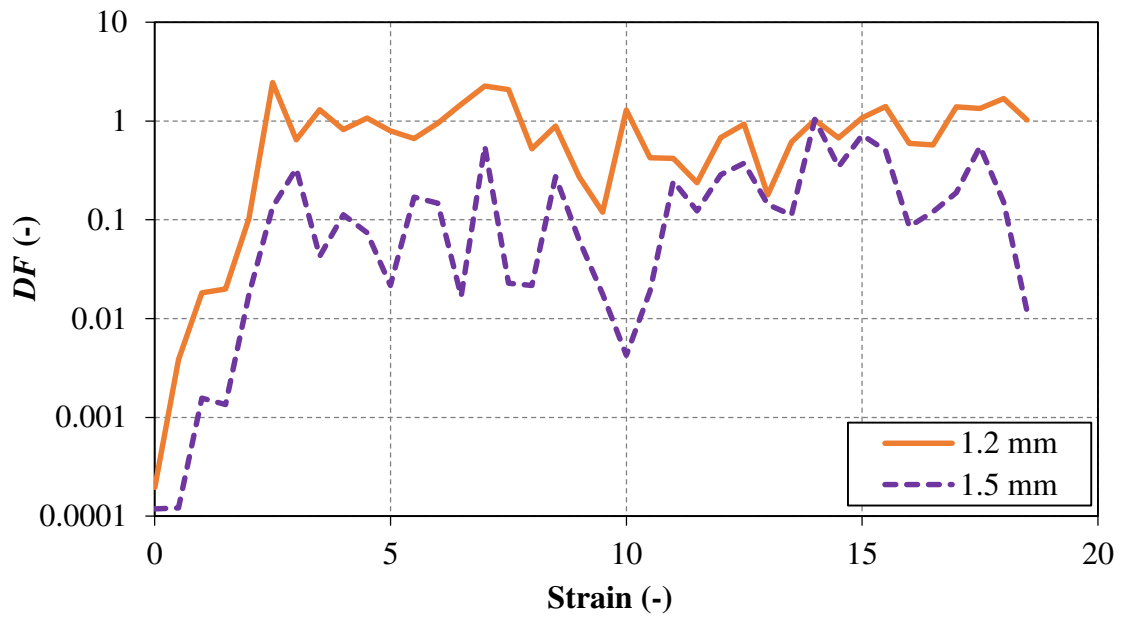
Fig. A6. DF as a function of strain for granule type C at gap sizes 1.5, 2.5, 2.7 and 3.1 mm.
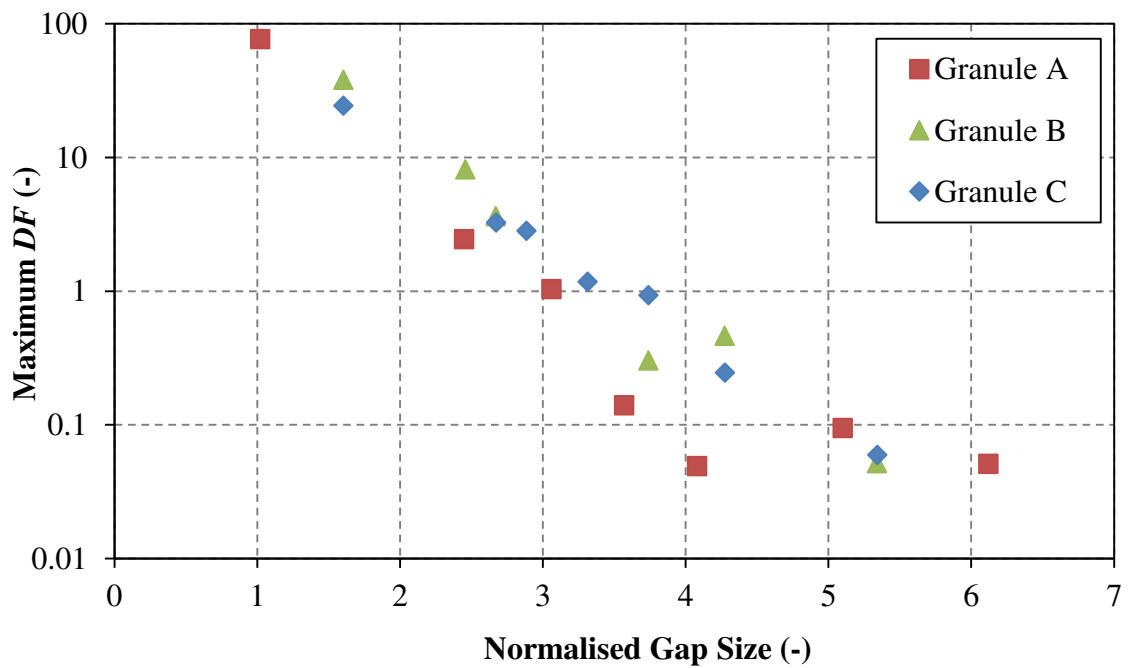
Analysis of Contact Force Distribution in a Moving Granule Bed Subjected to Shear Deformation by a Set of Rollers

FIGURES

Fig. 9. Illustration of the shear cell simulation.

2 mm gap, 13-21 rpm

Nip region

The particles included for calculation are those within the nip region of high stress (1 cm high).

0.11 m/s

Vxy

0 m/s
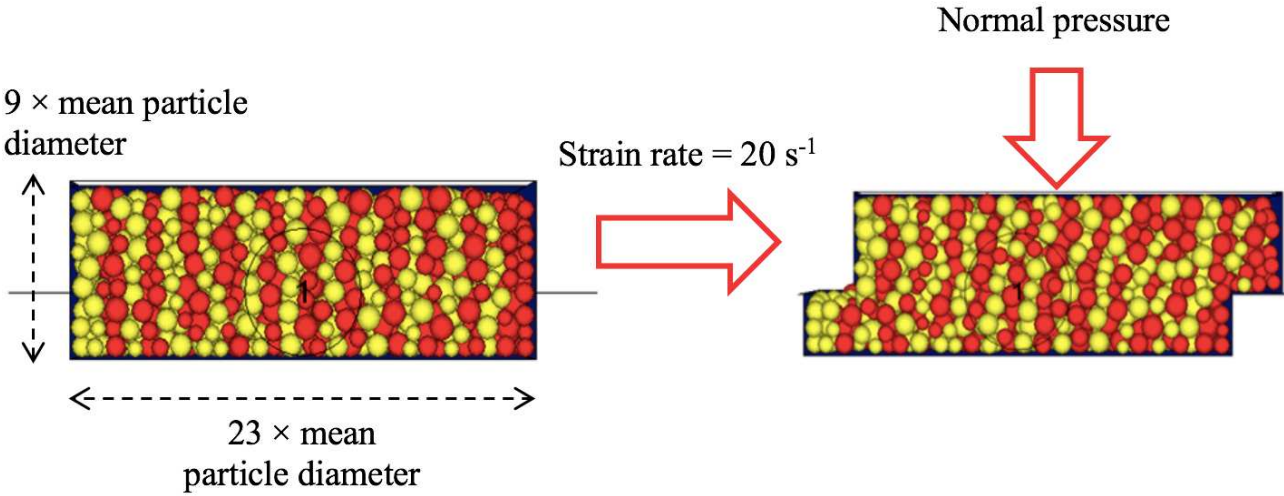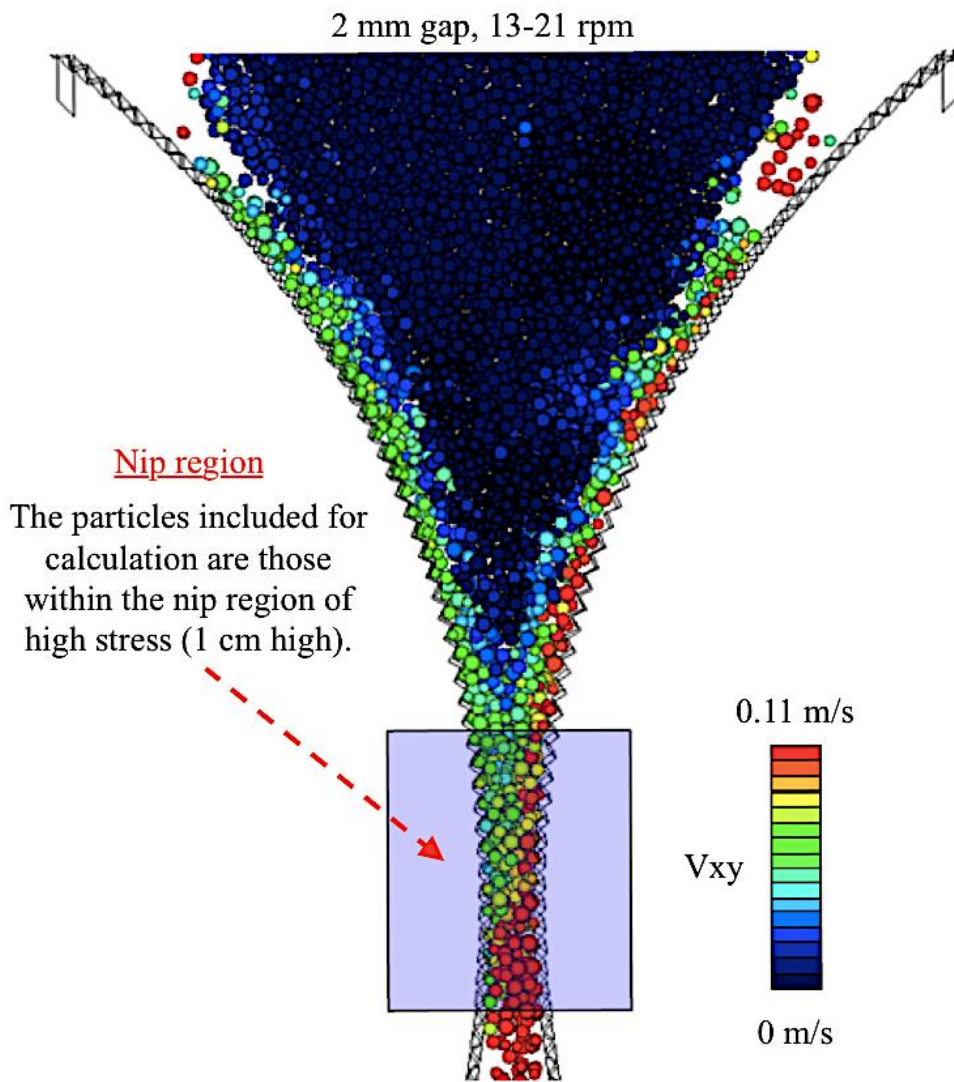
Fig. 10. Illustration of the roller simulation.
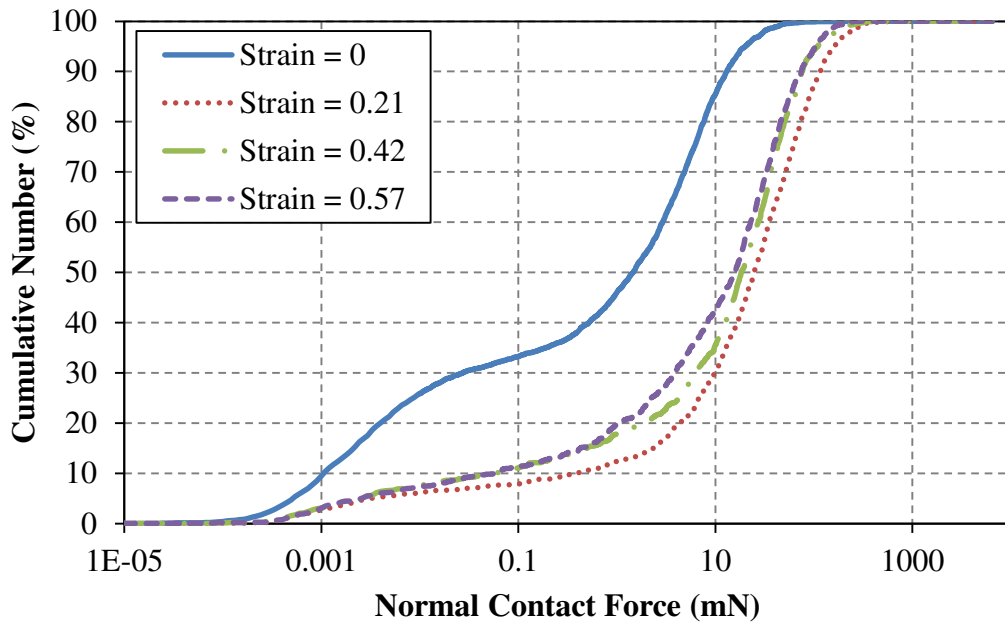
Fig. 11. Example of a typical shear cell normal contact force distribution.
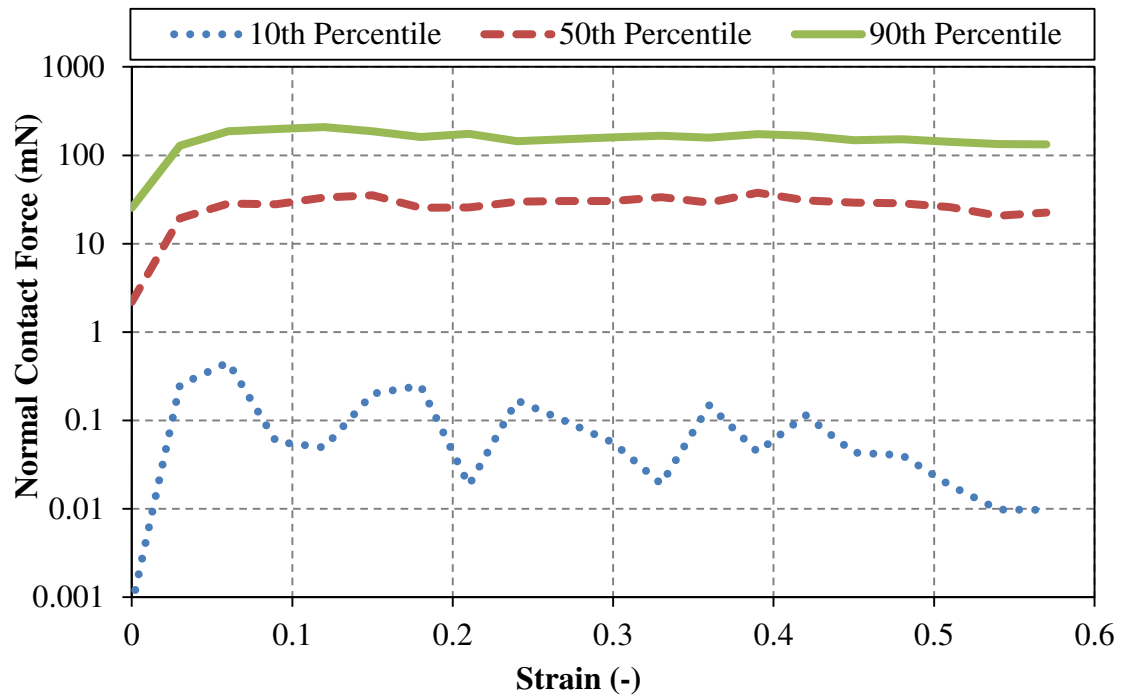

Fig. 12. The 10th, 50th and 90th percentiles of the normal contact force distribution in the shear cell as a function of strain for granule type A (normal stress = 13.1 kPa).

Fig. 13. The 10th, 50th and 90th percentiles of the normal contact force distribution in the rollers as a function of strain for granule type A (gap size = 1.5 mm).

Fig. 14. The 90th percentile of the normal contact force distribution in the rollers as a function of strain for granule type A for all the investigated gap sizes.

Fig. 15. *DF* as a function of strain for granule type A at gap sizes 1.2 and 1.5 mm.

Fig. 16. Maximum *DF* as a function of normalised gap size for all granule types.

APPENDIX

Fig. A7. The 10th, 50th and 90th percentiles of the normal contact force distribution in the shear cell as a function of strain for granule type B (normal stress = 14.7 kPa).
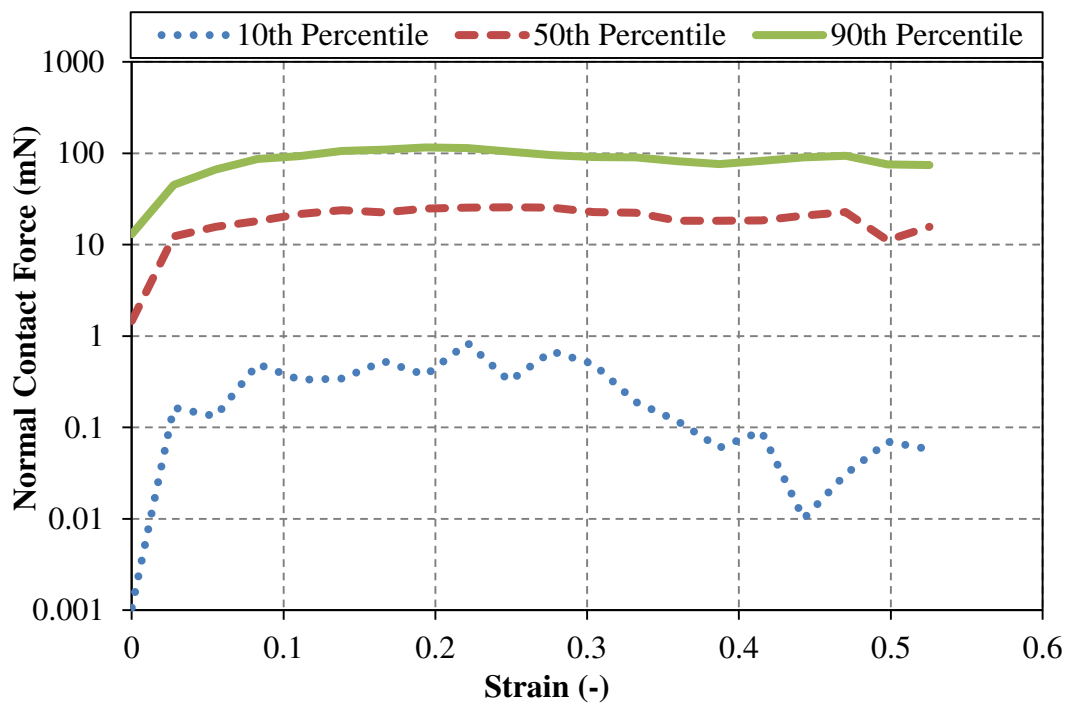

Fig. A8. The 10th, 50th and 90th percentiles of the normal contact force distribution in the shear cell as a function of strain for granule type C (normal stress = 8.4 kPa).
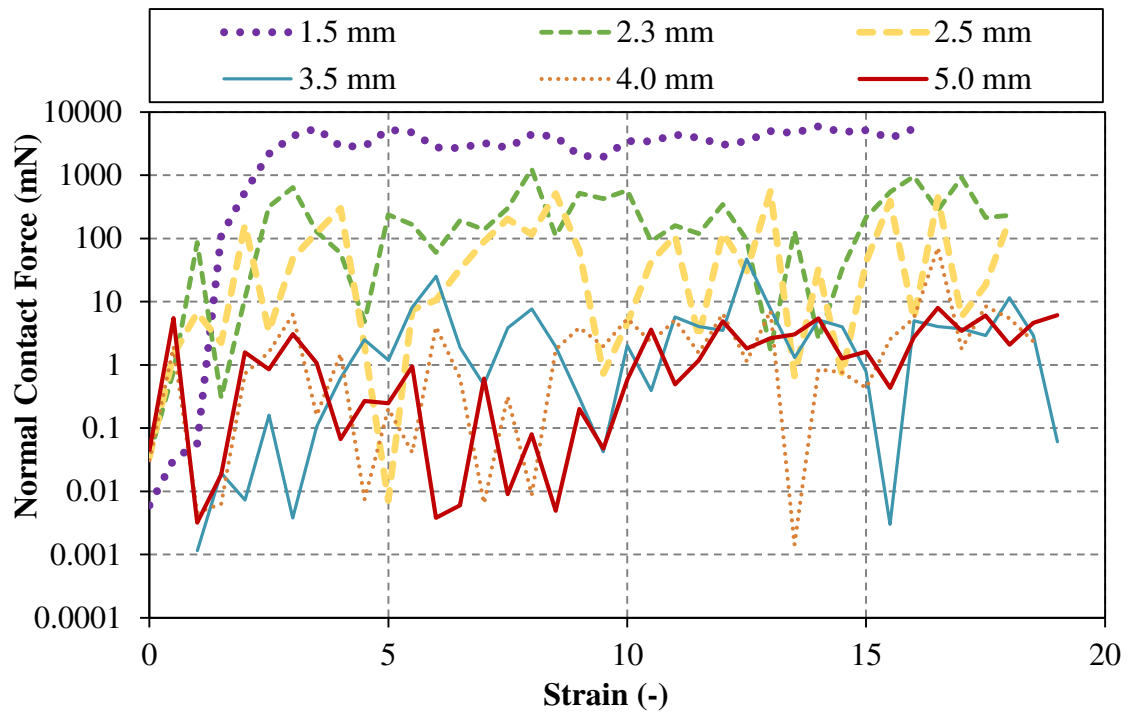
Fig. A9. The 90th percentile of the normal contact force distribution in the rollers as a function of strain for granule type B for all the investigated gap sizes.
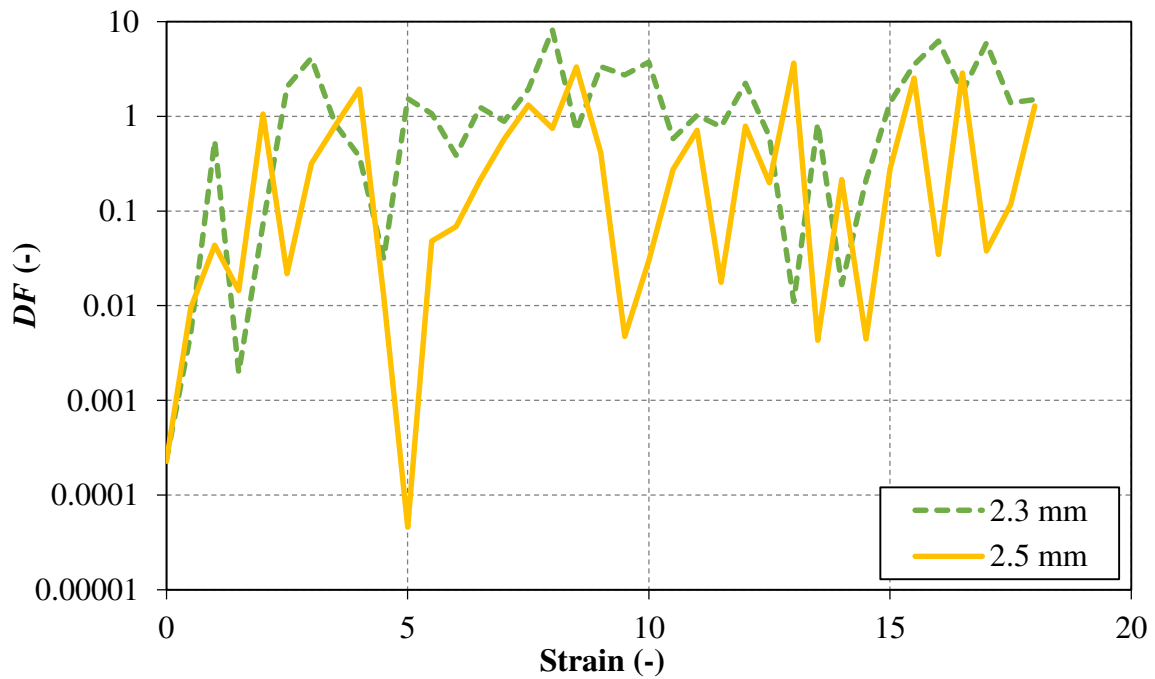

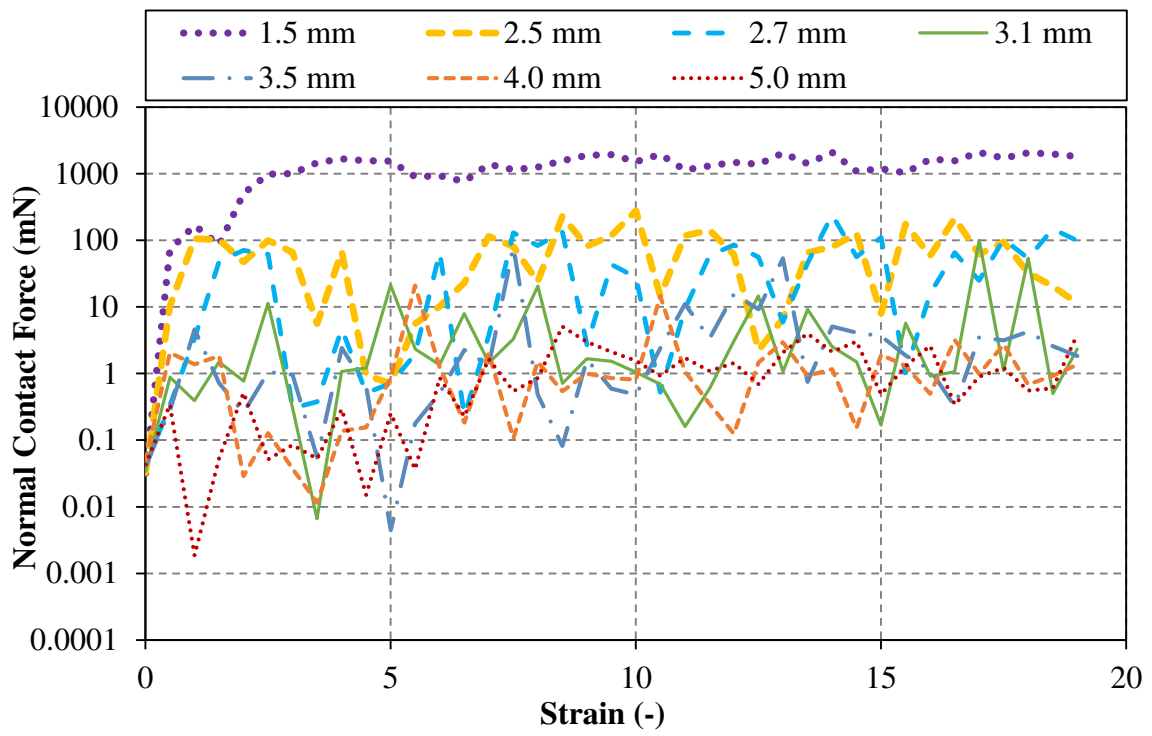Fig. A10. DF as a function of strain for granule type B at gap sizes 2.3 and 2.5 mm.

Fig. A11. The 90th percentile of the normal contact force distribution in the rollers as a function of strain for granule type C for all the investigated gap sizes.
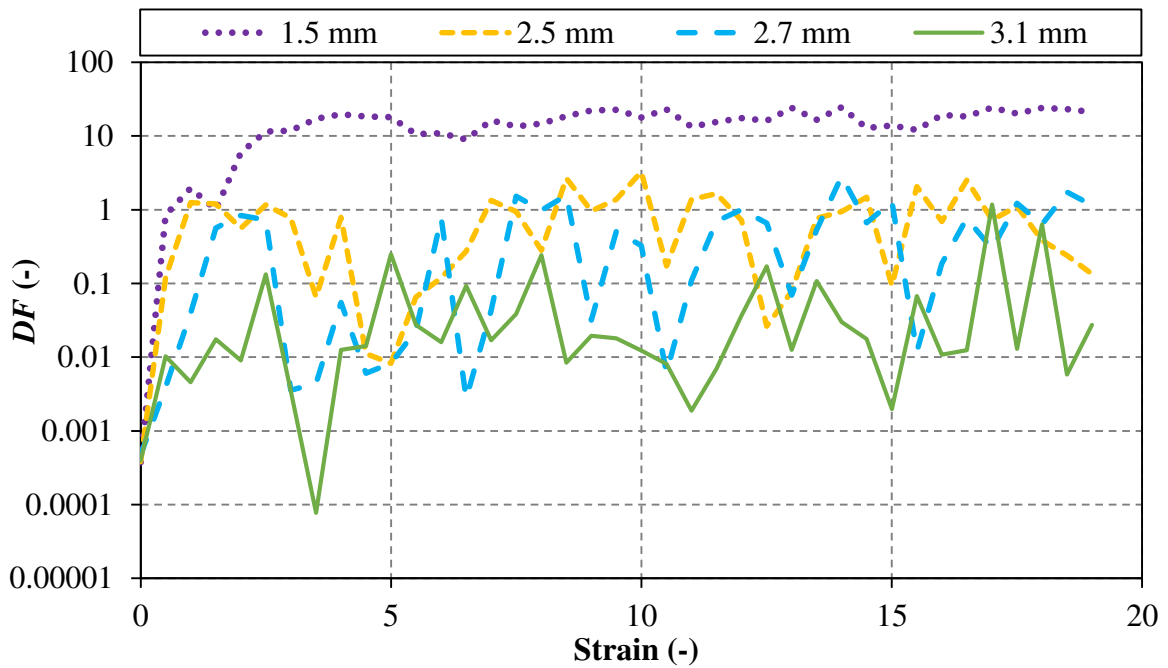

Fig. A12. DF as a function of strain for granule type C at gap sizes 1.5, 2.5, 2.7 and 3.1 mm.

Analysis of Contact Force Distribution in a Moving Granule Bed Subjected to Shear Deformation by a Set of Rollers

TABLES

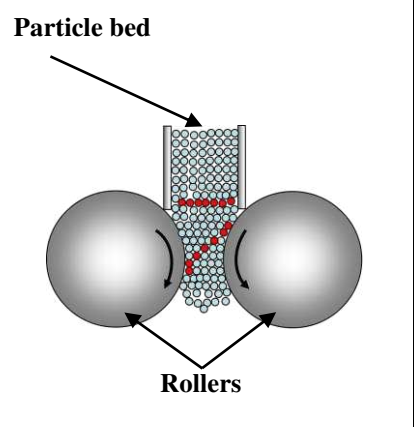Table 4. Description of the PSI tester rollers.

Schematic Diagram	Description
	Roller shearing: A dense particle bed is fed between two counter-rotating rollers with an adjustable gap, whilst the angular velocity of each roller can be set independently. The diameter and thickness of the rollers are 100 and 25.4 mm, respectively. The roller speeds can vary from 1 to 100 rpm either in clockwise or anticlockwise direction. The roller gap can be varied from 0.2 to 6 mm. The surface of the rollers is grooved (90°) with 1 mm pitch longitudinal corrugations. The gap between the rollers should be less than about six particles to effectively shear the bed as particles flow due to gravity [22] but larger than 2.2 particles to avoid crushing of individual particles [23]. It has previously been shown that shearing occurs in the nip region of the rollers.

Table 5. Shear cell simulation parameters and particle properties.

Granule Type	A	B	C	Wall
Particle Diameter (mm)	0.30 – 0.51	0.30 – 1.00	0.36 – 1.01	-
Number of Particles (-)	1800	1800	1800	-
Particle Density (kg/m³)	1550	1600	1280	-
Sliding Friction (-)	0.7	0.7	0.7	0.35
Rolling Friction (-)	0.2	0.2	0.2	-
Stiffness (N/m)	5×10^4	9×10^4	3×10^4	1×10^8
Coefficient of Restitution (-)	0.5	0.5	0.5	-
Target Normal Stress (kPa)	13.1	14.7	8.4	-

Table 6. The 90th percentile of the contact force distribution for granule types A, B and C subjected to normal loads of 13.1, 14.7 and 8.4 kPa, respectively.

Granule Type	90th Percentile of The Contact Force Distribution (mN)
A	30
B	180
C	100